

**FINDING TEMPERATURES AND HEAT FLUXES ON INACCESSIBLE  
SURFACES IN 3-D COATED ROCKET NOZZLES**

T. J. Martin and G. S. Dulikravich  
Department of Aerospace Engineering  
The Pennsylvania State University  
University Park, PA 16802

**ABSTRACT**

We have developed a new algorithm that uses the boundary element method (BEM) for determining thermal boundary conditions on surfaces of conducting three-dimensional solids where such quantities are unknown. The problem is solved by providing both temperature and heat flux on a surface where such data is readily available and then non-iteratively determining the temperature field within the object and any unknown thermal boundary conditions on the surfaces where thermal boundary values are unavailable. A three-dimensional steady-state inverse BEM computer program has been developed and was tested on a simple geometry where the analytic solution of the well-posed problem is known. The method has been applied to more complex three-dimensional geometries, including rocket thrust chamber walls with coolant passages and multiple thermal barrier coatings. The accuracy and reliability of this technique tends to deteriorate when the known surface conditions are only slightly over-specified and given far from the inaccessible surfaces.

**INTRODUCTION**

Often it is very difficult and even impossible to place sensors and take measurements of temperatures and heat fluxes on certain surfaces of a heat conducting solid due to the geometric inaccessibility of the surfaces or severity of the environment on these surfaces. These unknown thermal boundary values may be deduced from additional temperature or heat flux measurements made within the solid or on some other surfaces of the solid that are accessible. In the steady boundary condition inverse heat conduction problem (SIHCP), both temperature,  $T$ , and normal temperature derivative,  $Q$ , must be specified on a part of the solid's surface, while both  $T$  and  $Q$  are unknown on another part of the surface. Elsewhere on the solid's surface we should provide either  $T$ 's or  $Q$ 's. The surface section where both  $T$  and  $Q$  are specified simultaneously is called the over-specified boundary and is essential for solving the inverse problem. Our computational method<sup>1-6</sup> for solving these inverse problems is non-iterative and it has been shown to compute meaningful thermal fields in a single matrix inversion using a straight-forward modification to the standard boundary element method (BEM) analysis code.

**STEADY-STATE HEAT CONDUCTION**

The governing equation for the steady-state heat conduction of temperature,  $T(\mathbf{x})$ , in a solid isotropic domain  $\Omega$  bounded by the boundary  $\Gamma$  is given by

$$\nabla \cdot [k \nabla T(\mathbf{x})] = 0$$

Here,  $k$  is the coefficient of thermal conductivity and  $\mathbf{x}$  is the position vector. This elliptic partial differential equation of Laplace type can be subject to the Dirichlet (temperature  $T = u$ ) boundary conditions on the boundary  $\Gamma_1$ , the Neumann (heat flux  $-k \frac{\partial T}{\partial n} = Q$ ) boundary conditions on the boundary  $\Gamma_2$ , and, when a boundary is exposed to a moving fluid, the Robin (convective heat transfer  $-k \frac{\partial T}{\partial n} = h(T - T_{amb})$ ) boundary conditions on the boundary  $\Gamma_3$ . Here,  $n$  is the direction of the outward normal to the boundary  $\Gamma = \Gamma_1 + \Gamma_2 + \Gamma_3$ ,  $h$  is the convective heat transfer coefficient, and  $T_{amb}$  is the ambient fluid

temperature. The domain  $\Omega$  may be subdivided into a number of subdomains  $\Omega_1, \Omega_2, \dots, \Omega_M$ , each with a different coefficient of thermal conductivity. The solutions to the partial differential equation for each subdomain are combined using the compatibility relations on the interface boundaries, equating temperatures and heat fluxes. For example, for the interface between the subdomains  $\Omega_1$  and  $\Omega_2$ , the compatibility relations are

$$T_{11} = T_{12} \quad \text{and} \quad -k_{11} \left( \frac{\partial T}{\partial n} \right)_{11} = k_{12} \left( \frac{\partial T}{\partial n} \right)_{12}$$

where the subscript,  $l$ , refers to the interface boundary between the subdomains.

## BOUNDARY ELEMENT METHOD

The Boundary Element Method (BEM) is a very efficient numerical technique<sup>7</sup> for solving linear boundary value problems, although it is also capable of solving nonlinear problems such as viscous fluid flow, heat conduction with radiation, moving boundary problems such as solidification and melting, conjugate heat transfer, and other phenomenon. The BEM has been chosen to solve most of our inverse heat conduction problems because it has certain distinct advantages over the more common finite element or finite difference methods. The BEM is a non-iterative and direct solution procedure which, when used for linear boundary value problems with a relatively small number of subdomains, is significantly faster and more robust than the other numerical solution techniques. Analytic solution to the partial differential equation, in the form of the Green's function, is part of the BEM solution. Therefore, high accuracy is expected with the BEM because introducing the Green's functions does not introduce any error into the solution. This is valuable especially in the solution of inverse problems where high numerical accuracy is required. With the BEM the dimensionality of the problem is reduced by one order such that the unknowns are strictly confined to the boundaries,  $\Gamma$ , of the domain,  $\Omega$ . This characteristic eliminates the need for the often extremely difficult task of generating an internal boundary-conforming computational grid. And finally, the non-iterative nature of the BEM eliminates stability, reliability and convergence problems.

When a partial differential equation is formulated numerically, an approximate solution, which is, in general, not the exact solution, must be used. Therefore, error, often called the residual, is introduced into problem. The weighted residual statement minimizes this error by setting the weighted sum of the residuals over the entire domain and in the boundary conditions to zero. For Laplace's equation, the weighted residual statement appears as

$$\int_{\Omega} \left( \nabla^2 u(\mathbf{y}) \right) w(\mathbf{x}, \mathbf{y}) d\Omega(\mathbf{y}) + \int_{\Gamma_1} (u(\mathbf{y}) - \bar{u}(\mathbf{y})) \frac{\partial w(\mathbf{x}, \mathbf{y})}{\partial n} d\Gamma(\mathbf{y}) - \int_{\Gamma_2} (q(\mathbf{y}) - \bar{q}(\mathbf{y})) w(\mathbf{x}, \mathbf{y}) d\Gamma(\mathbf{y}) = 0$$

where  $w(\mathbf{x}, \mathbf{y})$  is an arbitrary weighting function,  $\mathbf{x}$  is the real space coordinate and  $\mathbf{y}$  is the coordinate of integration. The first integral in the weighted residual statement can be integrated by parts twice.

$$\int_{\Omega} \left( \nabla^2 u \right) w d\Omega = \int_{\Omega} \left( \nabla^2 w \right) u d\Omega + \int_{\Gamma} \frac{\partial u}{\partial n} w d\Gamma - \int_{\Gamma} \frac{\partial w}{\partial n} u d\Gamma$$

We can use the weighted residual statement to reduce the partial differential equation to an ordinary differential equation in the transformed space by choosing an appropriate weighting function. The solution corresponding to an applied potential concentrated at a point is frequently used in boundary value problems. In the BEM, the fundamental solution, which will be represented by  $u^*$ , replaces the weighting function,  $w$ . The fundamental solution is a function of only the distance between the source point,  $\mathbf{y}$ , and the observation point,  $\mathbf{x}$ . For the three-dimensional Laplace's equation with a unit source applied at the coordinate  $\mathbf{y}$ , the auxiliary Green's function solution equation, which governs the weighting function, is

$$\nabla^2 w + \delta(\mathbf{x} - \mathbf{y}) = \frac{d^2 u^*}{dr^2} + \frac{2}{r} \frac{du^*}{dr} + \delta(r) = 0$$

where the radial coordinate,  $r$ , is the distance from the source point to the observation node,  $r = |\mathbf{x} - \mathbf{y}|$ . Taking into consideration that, at the observation node, the governing equation for  $u^*$  equals the Dirac delta function, the following Boundary Integral Equation (BIE) is obtained

$$c(\mathbf{x}) u(\mathbf{x}) + \int_{\Gamma} q^*(\mathbf{x}, \mathbf{y}) u(\mathbf{y}) d\Gamma = \int_{\Gamma} u^*(\mathbf{x}, \mathbf{y}) q(\mathbf{y}) d\Gamma$$

$$\text{where } q = \frac{\partial u}{\partial n} \quad \text{and} \quad q^* = \frac{\partial u^*}{\partial n}$$

The fundamental solution for the three-dimensional Laplace's equation is  $u^* = \frac{1}{4\pi r}$ . The boundary,  $\Gamma$ , of an arbitrary multiply-connected domain,  $\Omega$ , can be discretized into  $N_{sp}$  boundary elements connected between  $N$  boundary nodes. One BIE can be constructed for every boundary node under consideration. The BEM solution set can then be constructed by integrating one BIE per boundary node. The resulting BEM solution set contains  $N$  equations with heat functions,  $u$ , and fluxes,  $q$ , unknown on the boundary only.

$$c_i u_i + \sum_{k=1}^{N_{sp}} \int_{\Gamma_k} q^* u d\Gamma = \sum_{k=1}^{N_{sp}} \int_{\Gamma_k} u^* q d\Gamma$$

The variation of  $u$  and  $q$  can be assumed to be constant, linear, quadratic, etc. on each boundary element. The points where the values of temperature and flux are  $u_{k,j}$  and  $q_{k,j}$  are called nodes. Since the nodes must also define the boundary discretization, the subscripts  $k$  refers to the boundary element and the  $j$  index indicates the element vertices (or element endpoints).

We have chosen to use bilinear isoparametric quadrilateral panels to represent the boundary elements discretizing the surface  $\Gamma$  of the three-dimensional domain,  $\Omega$ . After substitution, the whole BEM solution set can be represented in the following matrix form as

$$\begin{Bmatrix} c_1 u_1 \\ M \\ c_N u_N \end{Bmatrix} + \begin{bmatrix} h_{1,1} & L & h_{1,N} \\ M & O & M \\ h_{N,1} & L & h_{N,N} \end{bmatrix} \begin{Bmatrix} u_1 \\ M \\ u_N \end{Bmatrix} = \begin{bmatrix} g_{1,1} & L & g_{1,N_{sp}} \\ M & O & M \\ g_{N,1} & L & g_{N,N_{sp}} \end{bmatrix} \begin{Bmatrix} q_1 \\ M \\ q_{N_{sp}} \end{Bmatrix}$$

The entries in the  $[h]$  matrix are coefficients of nodal temperatures which are shared by several surface panels since the nodes are at the corners of the quadrilaterals. The terms are factored together because the temperature field is single-valued and unique. This should not occur with the fluxes because of the multi-valued nature of the normal on surface panels which are connected at a sharp corner<sup>5</sup>. The normal derivatives on each surface panel are kept unique and, as such, the  $[g]$  matrix and the vector of fluxes,  $\{q\}$  contain  $4 \times 1$  vectors per entry

For a well-posed boundary value problem, every point on the boundary is given one Dirichlet, Neumann or Robin-type boundary condition. The free term is absorbed into the diagonal of the  $[h]$  matrix resulting in the following matrix representation

$$[h] \{u\} = [g] \{q\}$$

The computation of the free term can be simplified. Rather than computing the geometric internal angle at the  $i$ th boundary node, the diagonal of the  $[h]$  matrix can be computed implicitly by considering what would happen if the temperature was constant everywhere and no heat sources were present. In this instance, fluxes would be identically zero. The diagonal, being the only unknown term in this case, can be computed by summing the remaining terms in the BEM so that

$$h_{ii} = - \sum_{j=1}^N h_{ij}$$

In the well-posed steady state problems, the boundary conditions may be multiplied out and transferred to the right-hand-side to form a vector of knowns,  $\{F\}$ , while the left-hand side remains in the standard form  $[A]\{X\}$ . The equation set that will result has  $N$  unknowns and  $N$  equations. It is a system of linear algebraic equations that can be solved for the unknown vector  $\{X\}$  by any appropriate matrix solver. If temperatures are known at discrete locations within the solid, additional equations can be added to this set, one for each such additional control point.

When an ill-posed (inverse) problem is encountered, the matrix  $[A]$  becomes highly ill-conditioned. The proper solution to this ill-conditioned matrix can provide accurate results to various SHCIP's. The approach is somewhat similar, at least in theory, to selectively discarding eigenvalues and eigenvectors of a particular system of equations that tends to magnify errors. For example, if at two vertices of a quadrilateral surface panel both  $u = \bar{u}$  and  $q = \bar{q}$  are known while at the remaining two vertices neither quantity is known, the BIE equation set begins as

$$\begin{bmatrix} h_{11} & h_{12} & h_{13} & h_{14} \\ h_{21} & h_{22} & h_{23} & h_{24} \\ h_{31} & h_{32} & h_{33} & h_{34} \\ h_{41} & h_{42} & h_{43} & h_{44} \end{bmatrix} \begin{bmatrix} \bar{u}_1 \\ u_2 \\ \bar{u}_3 \\ u_4 \end{bmatrix} = \begin{bmatrix} g_{11} & g_{12} & g_{13} & g_{14} \\ g_{21} & g_{22} & g_{23} & g_{24} \\ g_{31} & g_{32} & g_{33} & g_{34} \\ g_{41} & g_{42} & g_{43} & g_{44} \end{bmatrix} \begin{bmatrix} \bar{q}_1 \\ q_2 \\ \bar{q}_3 \\ q_4 \end{bmatrix}$$

In order to solve this set, all of the unknowns will be collected on the right-hand side, while all of the knowns are assembled on the left. A simple algebraic manipulation yields the following set.

$$\begin{bmatrix} h_{12} & -g_{12} & h_{14} & -g_{14} \\ h_{22} & -g_{22} & h_{24} & -g_{24} \\ h_{32} & -g_{32} & h_{34} & -g_{34} \\ h_{42} & -g_{42} & h_{44} & -g_{44} \end{bmatrix} \begin{bmatrix} u_2 \\ q_2 \\ u_4 \\ q_4 \end{bmatrix} = \begin{bmatrix} -h_{11} & g_{11} & -h_{13} & g_{13} \\ -h_{21} & g_{21} & -h_{23} & g_{23} \\ -h_{31} & g_{31} & -h_{33} & g_{33} \\ -h_{41} & g_{41} & -h_{43} & g_{43} \end{bmatrix} \begin{bmatrix} \bar{u}_1 \\ \bar{q}_1 \\ \bar{u}_3 \\ \bar{q}_3 \end{bmatrix}$$

Since the vector on the right-hand side is known, it may be multiplied by its coefficient matrix to form a vector of knowns,  $\{F\}$ . The left-hand side remains in the form  $[A]\{X\}$ . Also, additional equations may be added to the equation set if, for example, temperature or heat flux measurements are known at certain locations within the domain. In general, the coefficient matrix  $[A]$  will be non-square and highly ill-conditioned. Most matrix solvers will not work well enough to produce a correct solution. But, there exist appropriate techniques for dealing with sets of equations that are either singular or very close to singular. These matrix solution techniques, known as Singular Value Decomposition (SVD) methods<sup>8</sup>, are widely used in solving most linear least squares problems.

## NUMERICAL RESULTS

The three-dimensional BEM formulation for SIHCP was verified<sup>6</sup> on a configuration consisting of a spherical cavity concentrically located inside a solid sphere. Nothing was assumed to be known on the cavity surface, while both temperature and heat flux were enforced on the sphere surface. The results were very good despite the surface grid singularities at the poles of the sphere and the spherical cavity

Our three-dimensional SIHCP code was then exercised on a realistic engineering problem with multiple regions having different heat conductivities. High pressure, reusable rocket thrust chambers encounter progressive thinning<sup>9</sup> of the coolant passage wall after repetitive engine operation. This deformation is caused by high thermal plastic strains that eventually cause cracks to form in the coolant passage wall. An engineer may obtain experimental data such as shroud temperatures and heat fluxes, compressive strains and thrust chamber total pressure and temperature. Unfortunately, the engineer cannot obtain data within coolant flow passages imbedded<sup>9</sup> in the wall of the chamber due to the extremely low temperature of the liquid hydrogen coolant and the small dimensions of the passages. A circumferentially-periodic section of the thrust chamber wall and a coolant passage was used as a test case for the three-dimensional SIHCP where temperatures and heat fluxes on the walls of the coolant flow passage were treated as unknown. The hot gas wall was specified with a heat flux  $Q_{hot} = -100 \times 10^6$  W/m<sup>2</sup>. The outer boundary temperature of  $T_{outer} = 140$  K was taken from experimental measurements<sup>9</sup>. The circumferential periodicity of the 72 cooling passages was assumed to exist. Consequently, meridional boundaries of the chamber wall section were specified to be adiabatic  $\frac{\partial T}{\partial \theta} = 0.0$ . Similarly, front and end walls of the periodic chamber section were assumed to be adiabatic, that is  $(\frac{\partial T}{\partial x})_{front} = (\frac{\partial T}{\partial x})_{back} = 0.0$ . The chamber was 0.154 m long and the remaining dimensions and shapes can be seen in Figure 1. Liquid hydrogen was assumed to have an average bulk temperature of  $T_{amb} = 50$  K and the constant heat convection coefficient  $h_{hole} = 1 \times 10^5$  W m<sup>-2</sup> K<sup>-1</sup> was specified on the coolant flow passage. Several different material combinations and computational grid refinements were used to create test cases.

	Zirconium-oxide	Nickel-chromium	Copper	Copper closeout
Thermal conductivity k (W/m K)	8.0	23.0	378.0	385.0

Table 1 Thermal conductivities of different material layers used in the simulation

### ONE-MATERIAL CONFIGURATION

The well-posed (direct or analysis) problem was formulated where the constant heat convection coefficient  $h_{hole}$  was specified on the coolant flow passage walls,  $Q_{hot}$  was specified on the hot gas wall,  $T_{outer}$  was specified on the outer surface of the chamber, and  $(\partial T / \partial \theta) = 0.0$  on the meridional periodic surfaces. The BEM code solved this analysis problem in a fraction of a second on Cray-C90. The computed surface isotherms are depicted in Figure 2a. Then, an ill-posed (inverse) problem was created by pretending that nothing is known on the walls of the cooling passage, while enforcing on the hot gas surface both the already known  $Q_{hot}$  and the  $T_{hot}$  that was obtained from the analysis solution. Similarly, overspecified data was provided at the outer surface of the chamber by enforcing an already known  $T_{out}$  and the  $Q_{out}$  that was obtained from the analysis solution. Our BEM code solved this ill-posed problem (Fig. 2b) in a fraction of a second on a Cray-C90 computer. The comparison of the computed

surface isotherms from the direct and inverse BEM shows a reasonably good agreement despite the coarse grid used in this test case.

### THREE-MATERIAL CONFIGURATION

Next, the same test case was repeated with a thin layer of zirconium-oxide and a thin layer of nickel-chromium coating the hot gas surface of the thrust chamber. Isotherms computed by the well-posed (Fig. 3a) and the ill-posed (Fig. 3b) problem indicating good accuracy of our SIHCP algorithm.

### FOUR-MATERIAL CONFIGURATION

A complete model of the actual thrust chamber wall section (Fig. 1) was then analyzed<sup>9-10</sup> with four regions having different thermal conductivities (Table 1). Surface isotherms computed for the well-posed problem (Fig. 4a) and the ill-posed problem (Fig. 4b) indicate good agreement. Notice that a refined surface grid was used in this test case.

### FIN-IN-A-CHANNEL CONFIGURATION

Next, a thick fin shaped like a sine-wave was added to the inner hot wall of the coolant passage. The thrust chamber was made of four regions with different thermal conductivities. The predicted isotherms for the well-posed problem with this finned configuration (Fig. 5a) and for the ill-posed problem with the same configuration (Fig. 5b) compare well. This test case also demonstrates that even a seemingly minor shape alteration can produce a significant decrease of the temperature on the hot side of the coolant passage and that it can spread the isotherms, thus reducing the thermal stress concentration.

## CONCLUSIONS

We have recently developed a new method that has the capability to determine thermal boundary conditions (temperatures and heat fluxes) on surfaces of three-dimensional conducting solids where such quantities are unknown. The method is extremely fast since it uses a non-iterative direct approach based on boundary integral method in solving steady-state inverse heat conduction problems of unknown boundary condition type. This means that given any over-specified thermal boundary conditions (such as temperatures and heat fluxes on surfaces where such data are readily available) the algorithm computes the temperature field within the object and any unknown thermal boundary conditions on surfaces where the thermal boundary values are unavailable. A 3-D steady-state BEM program has been developed to perform automatic non-iterative determination of both temperatures and heat fluxes on parts of the interior and exterior boundaries. Accuracy of the computer code was tested on several simple geometries where the analytic solution for steady heat conduction was known. Results obtained were in good agreement with the analytic values in the regions relatively close to the overspecified data, but deteriorated with the distance from the overspecified boundaries.

## ACKNOWLEDGMENTS

The authors are grateful for the computing time provided by NASA NAS facility at Ames Research Center. Special thanks are due Mr. Brian Dennis for his invaluable help with computer graphics.

## REFERENCES

1. Martin, T.J. and Dulikravich, G.S., A Direct Approach to Finding Unknown Boundary Conditions in Steady Heat Conduction, 5th Annual Thermal and Fluids Analysis Workshop, Ohio Aerospace Institute-NASA Lewis Research Center, Ed: D. Darling, Brookpark, OH, August 16-20, 1993, NASA CP-10122, pp. 137-149.
2. Martin, T.J. and Dulikravich, G.S., Inverse Determination of Temperatures and Heat Fluxes on Inaccessible Surfaces, 9th International Conference on Boundary Element Technology - BETECH 94,

Computational Mechanics Publications, Southampton, Editors: C. Brebbia and A. Kassab, Orlando, FL, March 16-18, 1994, pp. 69-76.

3. Martin, T.J. and Dulikravich, G.S., Finding Unknown Surface Temperatures and Heat Fluxes in Steady Heat Conduction, 4th Intersociety Conference on Thermal Phenomena in Electronic Systems, Editors: A. Ortega and D. Agonafer, Washington, D.C., May 4-7, 1994, pp. 214-221; also in *IEEE Transactions of Components, Packaging and Manufacturing Technology (CPMT) Society - Series A*, Vol. 18, No. 3, September 1995, pp. 540-545.
4. Dulikravich, G.S. and Martin, T.J., Inverse Problems and Design in Heat Conduction, 2nd IUTAM International Symposium on Inverse Problems in Engineering Mechanics, Editors: H.D. Bui, M. Tanaka, M. Bonnet, H. Maigre, E. Luzzato and M. Reynier, Paris, France, November 2-4, 1994, A.A. Balkema, Rotterdam, 1994, pp. 13-20, 1994.
5. Martin, T.J. and Dulikravich, G.S., Inverse Determination of Boundary Conditions in Steady Heat Conduction With Heat Generation, Symposiums on Conjugate Heat Transfer, Inverse Problems, and Optimization, and Inverse Problems in Heat Transfer, Ed: W. J. Bryan and J. V. Beck, ASME National Heat Transfer Conference, Portland, OR, August 6-8, 1995, ASME HTD-Vol. 312, pp. 39-46; also, to appear in *ASME Journal of Heat Transfer*, 1996.
6. Dulikravich, G.S. and Martin, T.J., Inverse Shape and Boundary Condition Problems and Optimization in Heat Conduction, Chapter no. 4 in *Advances in Numerical Heat Transfer* (editors: W.J. Minkowycz and E.M. Sparrow), Taylor and Francis, 1996.
7. Brebbia, C.A. and Dominguez, J., *Boundary Elements, An Introductory Course*, McGraw-Hill Book Company, New York, 1989.
8. Press, W.H., Teukolsky, S.A., Vetterling, W.T. and Flannery, B.P., *Numerical Recipes in FORTRAN*, Second Edition - Cambridge Univ. Press, 1992.
9. Quentmeyer, R.J., Thrust Chamber Thermal Barrier Coating Techniques, NASA TM-100933, October 1988.
10. Carlile, J.A. and Quentmeyer, R.J., An Experimental Investigation of High-Aspect-Ratio Cooling Passages, NASA TM-105679, July 1992; also AIAA paper 92-3154.

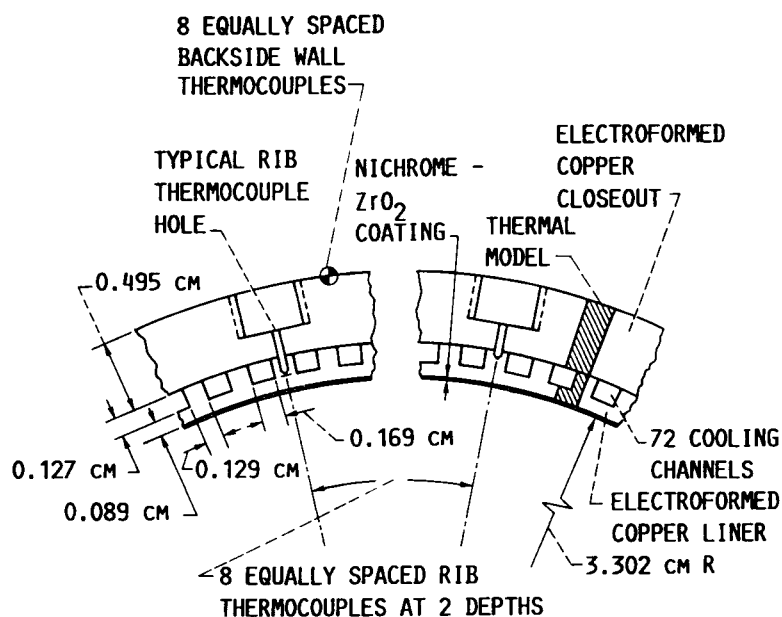
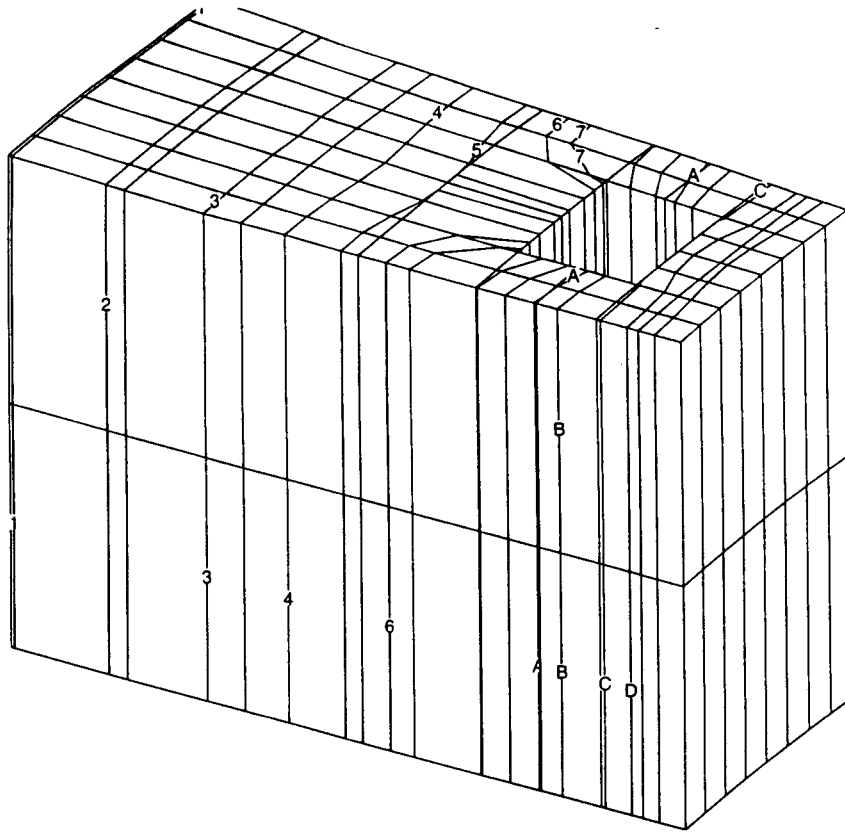
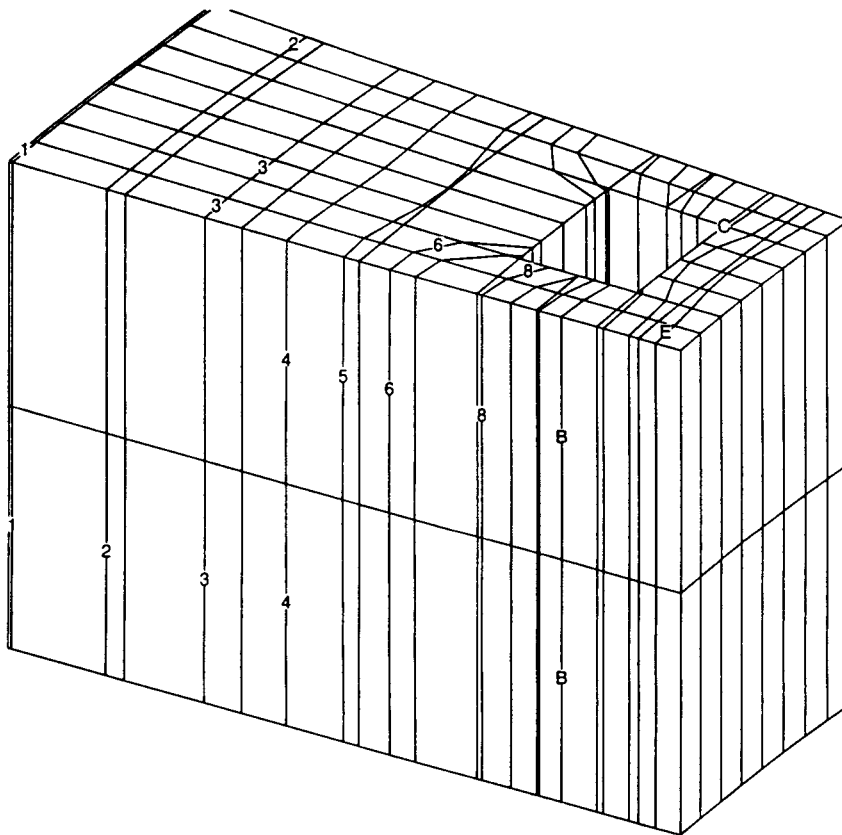


Fig. 1. Thrust chamber wall cross section showing instrumentation locations and dimensions



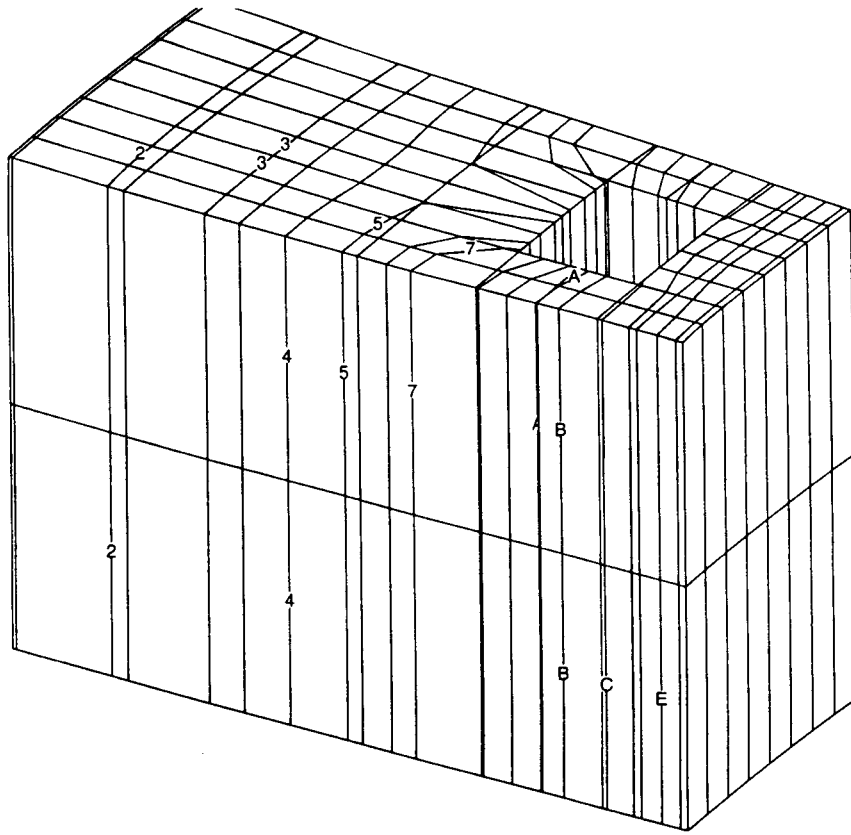
Level	$\theta$
F	1923.5
E	826.567
D	746.781
C	669.452
B	552.454
A	491.619
9	437.355
8	384.202
7	326.679
6	306.872
5	276.419
4	251.383
3	217.076
2	177.857
1	141.466



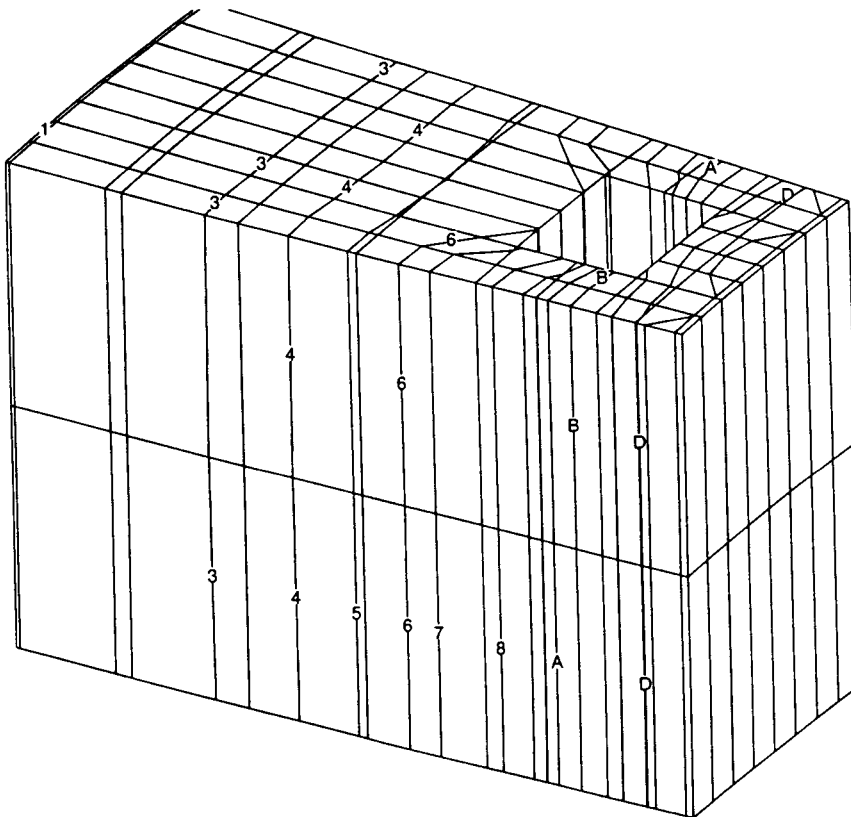
Level	$\theta$
F	1923.5
E	826.567
D	746.781
C	669.452
B	552.454
A	491.619
9	437.355
8	384.202
7	326.679
6	306.872
5	276.419
4	251.383
3	217.076
2	177.857
1	141.466

Fig. 2 One-material test case: computed surface isotherms for a) direct problem, b) inverse problem



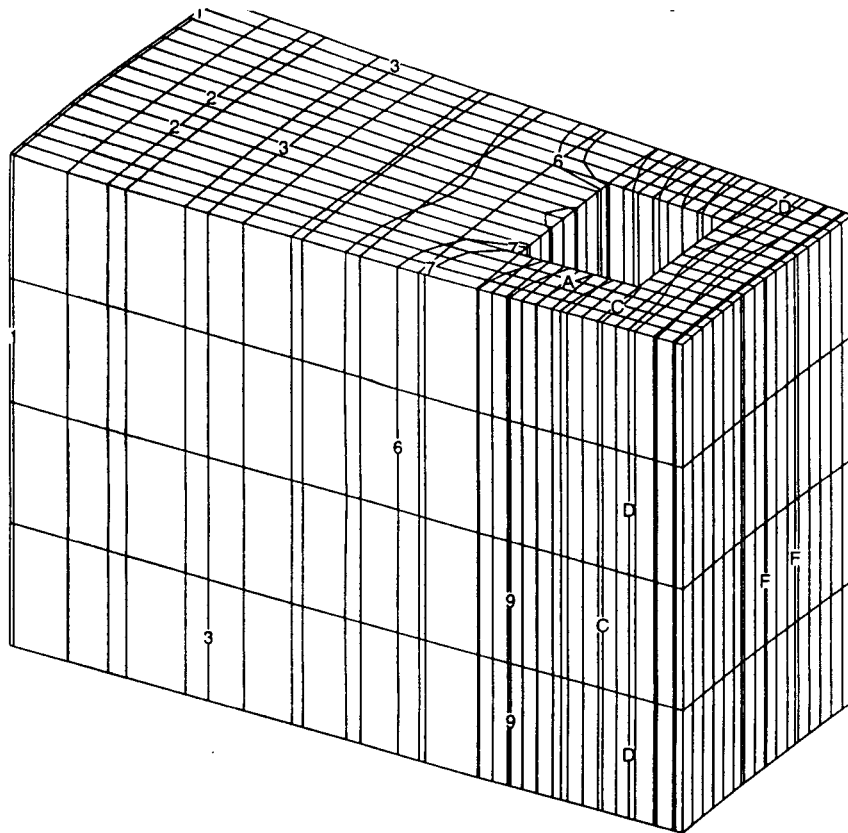


Level	$\theta$
F	1923.5
E	826.567
D	746.781
C	669.452
B	552.454
A	491.619
9	437.355
8	384.202
7	326.679
6	306.872
5	276.419
4	251.383
3	217.076
2	177.857
1	141.466

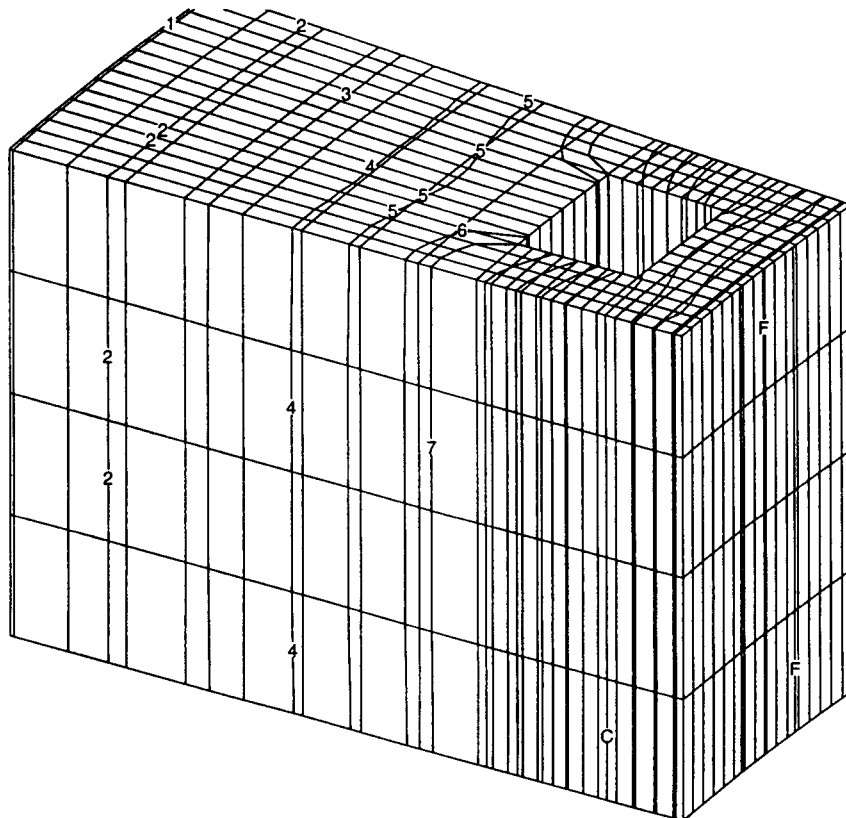


Level	$\theta$
F	1923.5
E	826.567
D	746.781
C	669.452
B	552.454
A	491.619
9	437.355
8	384.202
7	326.679
6	306.872
5	276.419
4	251.383
3	217.076
2	177.857
1	141.466

Fig. 3 Three-material test case: computed surface isotherms for a) direct problem, b) inverse problem

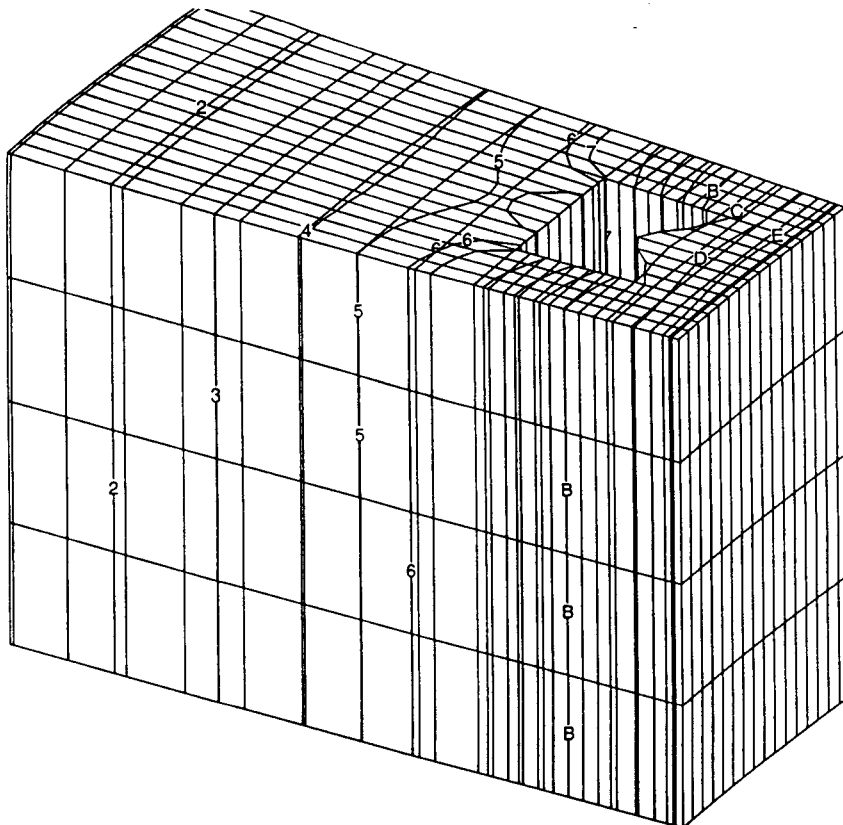


Level	$\theta$
F	1923.5
E	826.567
D	746.781
C	669.452
B	552.454
A	491.619
9	437.355
8	384.202
7	326.679
6	306.872
5	276.419
4	251.383
3	217.076
2	177.857
1	141.466

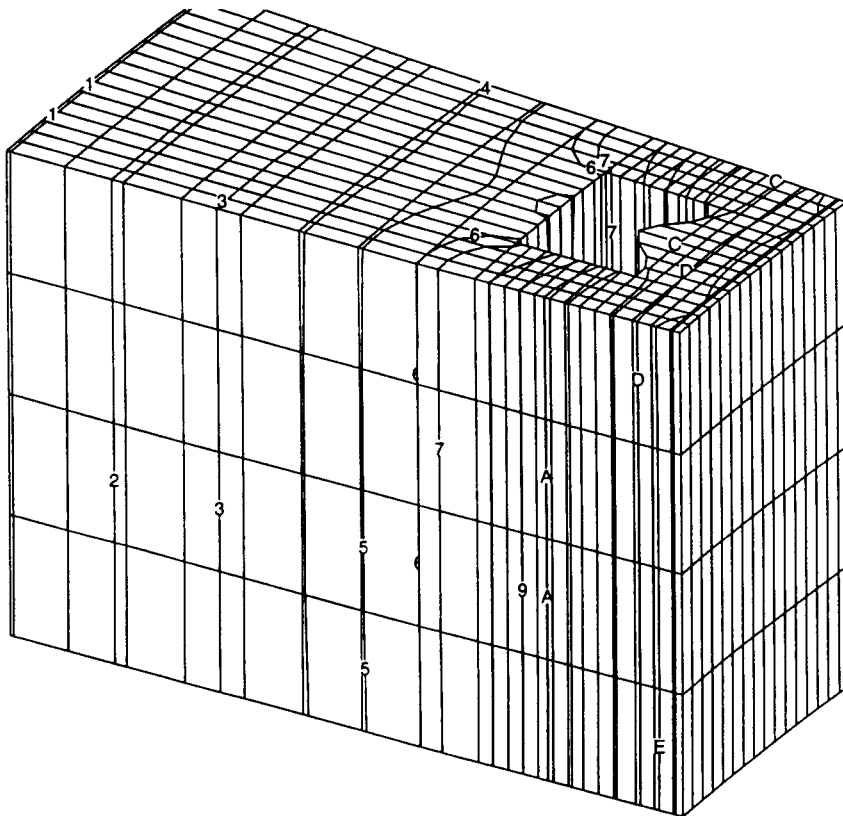


Level	$\theta$
F	1923.5
E	826.567
D	746.781
C	669.452
B	552.454
A	491.619
9	437.355
8	384.202
7	326.679
6	306.872
5	276.419
4	251.383
3	217.076
2	177.857
1	141.466

Fig. 4 Four-material test case: computed surface isotherms for a) direct problem, b) inverse problem



Level	$\theta$
F	1923.5
E	826.567
D	746.781
C	669.452
B	552.454
A	491.619
9	437.355
8	384.202
7	326.679
6	306.872
5	276.419
4	251.383
3	217.076
2	177.857
1	141.466



Level	$\theta$
F	1923.5
E	826.567
D	746.781
C	669.452
B	552.454
A	491.619
9	437.355
8	384.202
7	326.679
6	306.872
5	276.419
4	251.383
3	217.076
2	177.857
1	141.466

Fig. 5 Finned test case: computed surface isotherms for a) direct problem, b) inverse problem